ELSEVIER

Materials Science and Engineering B 141 (2007) 23–27

MATERIALS SCIENCE & ENGINEERING B

www.elsevier.com/locate/mseb

Improving the electrical conductance of chemically deposited zinc oxide thin films by Sn dopant

M.R. Vaezi *, S.K. Sadrnezhaad

Advanced Materials Research Center, Materials and Energy Research Center, Karaj, Iran

Received 31 August 2006; received in revised form 11 November 2006; accepted 26 May 2007

Abstract

The Sn-doped ZnO films produced from a zinc complex solution containing tin ions were deposited onto Pyrex glass substrates using a two-stage chemical deposition (TSCD) process. The experimental results show that the deposition rate increases linearly with Sn concentrations (atomic percent, at.%) when lower than 3% of them were used. Only the (0 0 2) X-ray diffraction 2θ peak appears in the range of this study. The incorporation of tin atoms into zinc oxide films is obviously effective, when Sn concentration is above 2.5%. The resistance of undoped ZnO films is high and reduces to a value of $4.2 \times 10^{-2}\ \Omega$ cm when 2.5% of Sn is incorporated. All of the zinc oxide films have above 80% transmittance in a range of 400–700 nm. The optical energy gap increases with the amount of Sn in the ZnO films.

Keywords: Conductance; ZnO films; Deposition; Doping; Transmittance

1. Introduction

Transparent and conductive oxide films, which are derivated from wide band-gap semiconductors with low specific resistance and high transparency in the visible wavelength range [1], have found wide applications in recent years. One of the most potential candidate substitutes for the ITO film being the ZnO. The structural characteristics, electrical and optical properties of the ZnO films have been widely investigated [2–4], while the doping effect on its properties is still under investigation. Most of these investigations focused on doping III A elements such as Al, Ga, In [5,6] and I A elements such as Li [7] and Na [8]. In this study, we chose Sn as the dopant because it becomes Sn^{4+} when it substitutes Zn^{2+} site in the ZnO crystal structure resulting in two more free electrons to contribute to the electric conduction. Furthermore, the radius difference between Sn^{4+} and Zn^{2+} is approximately 30% and it is possible to form a limited solid solution. Doped zinc oxide films have attracted much attention due to their great potential for application to transparent conducting electrodes [9,10] and insulating or creating ferroelectric layers [11] in opto-electronic devices.

There are numerous methods for the preparation of transparent conductive zinc oxide films, such as sputtering, electron beam evaporation [12,13], spray pyrolysis [14,15], MOCVD [16], electroless bath deposition [17], PLD [18] and chemical deposition [19,20]. Chemical deposition of thin films from aqueous solutions is a very promising method because of its simplicity and economy. The method mentioned here describes the deposition of ZnO film with a thickness and conductivity which can be controlled during the preparation procedure. Deposition is performed onto any substrate non-reactive with the chemicals used for deposition.

2. Experimental

Pyrex glass plates with 25 mm × 15 mm × 1 mm dimensions were used as the solid substrate for film growth. After degreasing, the plates were washed with de-ionized water and dried in hot steam. The final solution composition and the bath conditions that were used in this work are shown in Table 1. The zinc complex solution (having the composition shown in Table 1) was prepared by mixing concentrated NH_4OH with 0.2 M $ZnCl_2$ until white $Zn(OH)_2$ was precipitated. Further addition of NH_4OH resulted in the dissolving of the precipitate. The solution was diluted up to the appropriate concentration of Zn^{2+}. This was found to be the most convenient concentration

* Corresponding author. Tel.: +98 21 33555471; fax: +98 21 88773352.
E-mail addresses: vaezi9016@yahoo.com (M.R. Vaezi), sadrnezh@sharif.edu (S.K. Sadrnezhaad).

0921-5107/$ – see front matter © 2007 Elsevier B.V. All rights reserved.
doi:10.1016/j.mseb.2007.05.010

Table 1
Bath conditions and chemical deposition parameters with their various ranges for ZnO deposition

Variable	Range
$ZnCl_2$ (g l^{-1})	20–100
NH_3 (ml)	10–50
Tiron	4 drops/l
Sn (at.%)	0.5–3
pH	8–11
Temperature of complex solution (°C)	10–20
Temperature of hot water (°C)	90–105

for production of a good quality film on the substrate. Then, $SnCl_4$ (Merck, #780) with different concentrations was added to the prepared solution and stirred vigorously. Cleaned substrates were first immersed into a cold complex containing the solution and then in hot water for 2 s. After a required number of dipping, the substrate with the deposited ZnO film was annealed at 350 °C for several hours.

ZnO films produced in this work were characterized for their surface morphology, chemical composition, phases, and preferred orientation. The surface morphology was studied by scanning electron microscopy (SEM) using a Philips model MV2300 operated at 25 kV. The atomic percentage of Sn in the ZnO films was semi-quantitatively determined using the Kevex model energy dispersive X-ray spectroscopy (EDAX) system attached to the SEM. In order to verify the accuracy of the EDAX analysis, one deposit was also analyzed through wet chemistry using atomic absorption spectroscopy (AAS).

X-ray diffraction (XRD) was used to determine the phase present and the preferred orientation of the deposits. A Philips Xpert-Pro X-ray diffractometer with a Cu Kα radiation ($\lambda = 1.5418$ Å) was employed to obtain an XRD spectra using standard θ–2θ geometry. A computer-based search and match was used for phase identification.

A conventional stylus surface roughness detector (Alphastep 200) was used to measure the film thickness. All film thicknesses in this study were kept at a constant value. The resistivity of the films was measured by a four-point probe system (Napson, RT-7). The sheet resistivity was measured by a four-point probe machine and transformed to a resistivity combining with the value of film thickness.

3. Results and discussion

The effect of adding the Sn dopant and increasing the dipping number on the thickness of the deposited ZnO film is presented in Fig. 1. It can be seen that the doping process decreases the average deposition rate. The average deposition rate per dipping stage was estimated to be 0.012 and 0.008 μm for undoped and Sn-doped films, respectively. Fig. 1 shows that the relation between the thickness of the film is linear with the dipping number. The rate of increase in thickness is therefore constant. Unchanged solution concentration during the growing process seems to be responsible for this effect.

Fig. 2 shows the XRD spectra for the ZnO films doped with Sn at different concentrations of Sn dopant. It reveals that the

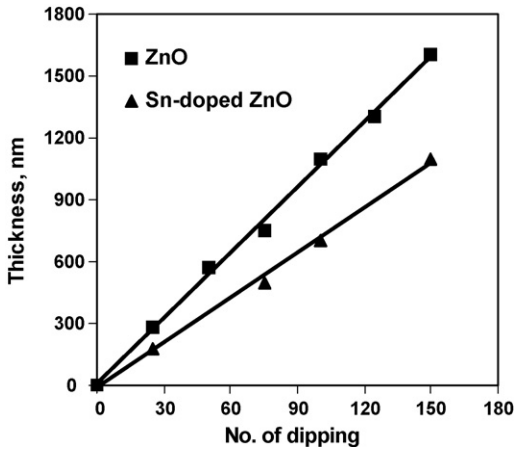

Fig. 1. Effect of number of dipping and Sn doping on ZnO film thickness.

deposited films produced with less than 2% of Sn are polycrystalline with (0 0 2) preferred orientation. This tendency is the same as our previous studies without dopant [21,22]. It is concluded that no matter how the Sn impurity is incorporated, the ZnO films always show the (0 0 2) preferred orientation. The (0 0 2) diffraction peak becomes obvious when 1.5% of Sn is added. However, the intensity of (0 0 2) is decreased to a lower value when the concentration of Sn dopant is further increased. This indicated that the ZnO films with Sn dopant produced at low concentration of Sn dopant have the tendency to show (0 0 2) preferred orientation but exhibit no obvious preferred orientation when the films are deposited at high concentrations of Sn dopant. The ZnO films produced at higher concentrations of Sn dopant may be weakly crystalline or even amorphous according to the data presented. The value of (0 0 2) diffraction peak obtained

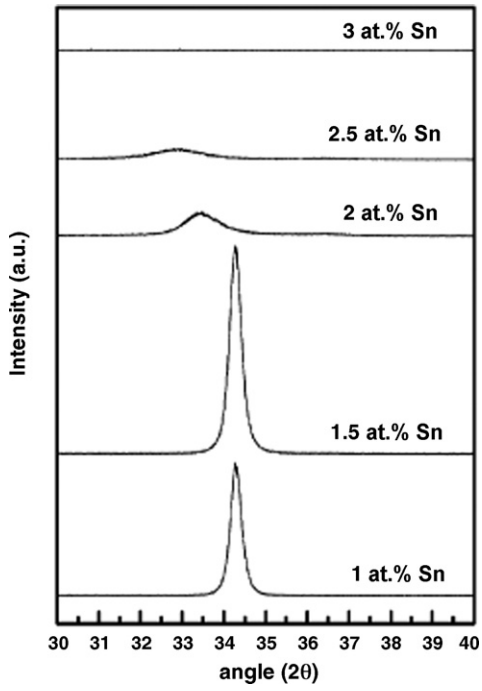

Fig. 2. XRD spectra for the ZnO:Sn thin films with different concentrations of Sn dopant.

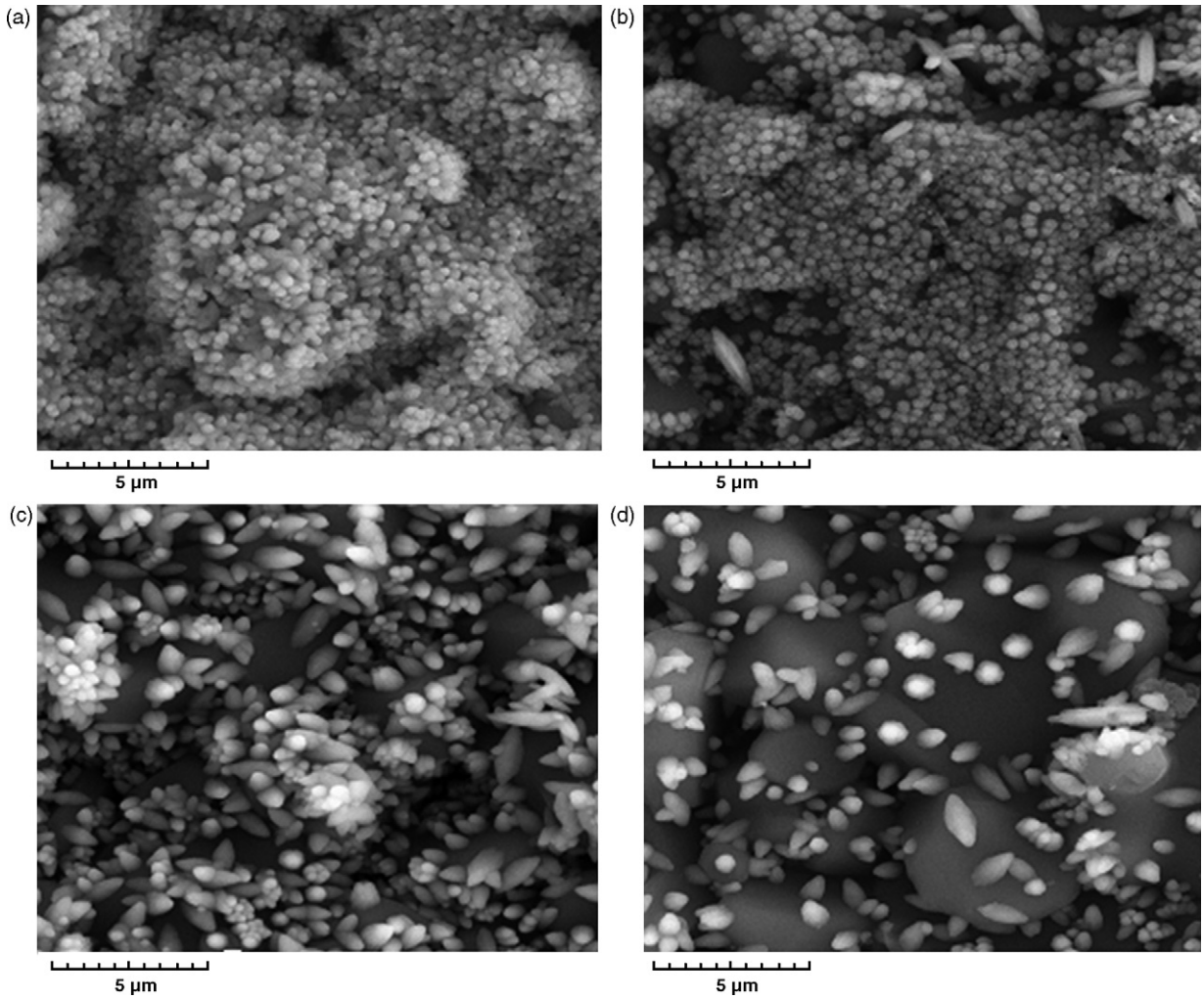

Fig. 3. SEM micrographs of Sn-doped ZnO thin films deposited after 100 times of dipping containing (a) 1% Sn, (b) 1.5% Sn, (c) 2.5% Sn and (d) 3% Sn.

in this study is very close to that of the standard ZnO crystal (34.5°). Neither SnO_2 nor Zn_2SnO_4 second phase is observed in the 20–60° (2θ) scanning range. This implies that tin atoms may replace zinc atomic sites or incorporate interstitially in the hexagonal lattices. Segregation of tin atoms to grain boundaries is less possible because the temperature is not high enough for tin to diffuse to grain boundaries in this study. After careful examination of the XRD patterns it can be found that the (0 0 2) peaks shift to a lower value when more than 2% of Sn is added to the solution. Furthermore, the peaks are broader and almost disappear when 3% of Sn is added. Because Sn atoms incorporated in the ZnO lattice induce a large residual stress in the films and result in the shifting of diffraction patterns. At high concentration of Sn dopant, the poisoning effect of nucleation stage increases destroying the well-established crystal structure of ZnO, which finally leads to a less crystalline structure.

Fig. 3 shows the effect of the addition of Sn dopant on morphology of the chemically deposited zinc oxide having a constant thickness (100 times of dipping). Less than a 2% Sn addition (e.g. 1%) prevents the growth of the zinc oxide nuclei. It poisons the deposit and prevents the growth process. An addition greater than 2% of Sn induces the poisoning of the nucleation stage and hinders fine grain formation. The same effect is observed in the addition of other surfactants [23]. With a dense/nodular-shape appearance, the film produced from the precursor of zinc complex containing 1.5% Sn is composed of ZnO particles in even sizes of 110–190 nm. At lower numbers of dipping, and lower thickness, the surface of the substrate is not completely covered with ZnO particles. Growth of the nuclei is therefore not observed. At a low number of dipping, Sn dopant does not significantly affect the morphology of the doped ZnO thin film formed on Pyrex substrate (Fig. 4).

As it is shown in Figs. 3 and 4, the surface morphology of all specimens is the same but their crystallite size is different. As the crystallite size decreases, the electrical conductance of thin film is improved [24–26]. Fig. 5 shows the variation of resistivity as a function of the atomic percent of Sn dopant. When comparing the resistivity of undoped ZnO thin films with Sn-doped ZnO thin films it is found that the resistivity decreases from a large value beyond detectable range to $2.1 \times 10^{-2}\,\Omega\,\text{cm}$ when 1% of Sn is added to the solution. The decrease in resistivity may be explained as follows: since the ionic radius of tin ($r_{Sn^{4+}} = 0.38$ Å) is smaller than that of the zinc ion ($r_{Zn^{2+}} = 0.6$ Å), the tin atoms doped into a ZnO lattice act as donors by supplying

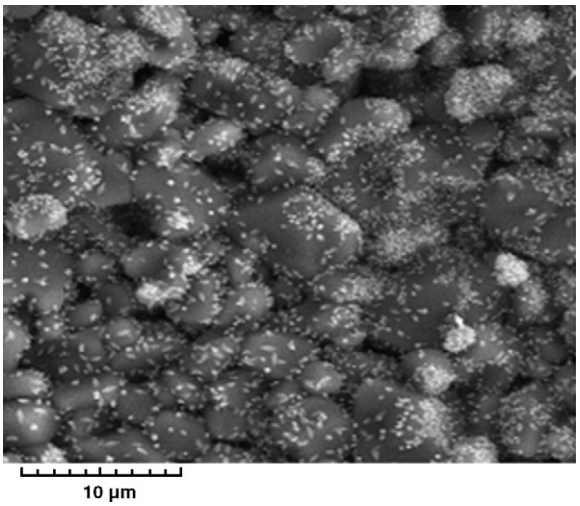

Fig. 4. SEM micrograph of Sn-doped ZnO thin films deposited after 30 times of dipping in a solution containing 1% Sn.

two free electrons when the Sn^{4+} ions occupy Zn^{2+} ion sites. This in turn increases the free carrier concentration and hence, decreases the resistivity. The mechanism of the conduction can be described by the following equation:

$$SnO_{2\,ZnO} \rightarrow Sn''_{Zn} + O^{x}_{O} + \tfrac{1}{2}O_2 + 2e'$$

Sn^{4+} ions substituted Zn^{2+} ions in the lattice induce positive Sn''_{Zn} charges in the material. In order to maintain electrical neutrality, two negative electrons are induced to compensate the excess positive charges. Hence the resistivity decreases due to increasing free electrons in the film. In the concentrations between 1 and 2% of Sn, little change of resistivity is found. However, when more than 2.5% of Sn was added, the resistivity suddenly increases one order of a magnitude. At higher concentrations, more Sn atoms can be effectively incorporated into the lattice of ZnO. On the other hand, the residual stress arises simultaneously as well. The stress field would reflect electric carriers and result in high resistivity.

The physics of defects in ZnO is quite complex and to a large extend unknown, and the understanding of doping and conduction mechanisms in this material are still incomplete and challenging. Thorough systematic studies of the mechanisms of electrical transport, and the effect of the interaction between defects and dopants on these mechanisms, are scarce [27–29].

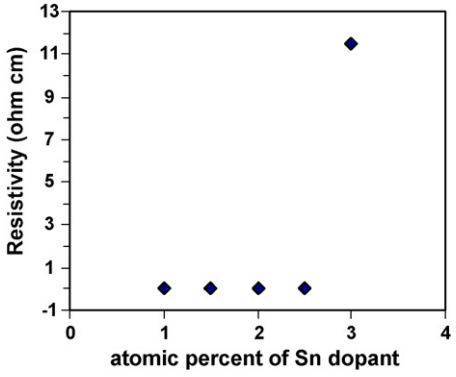

Fig. 5. Variation of resistivity as a function of concentration of Sn dopant.

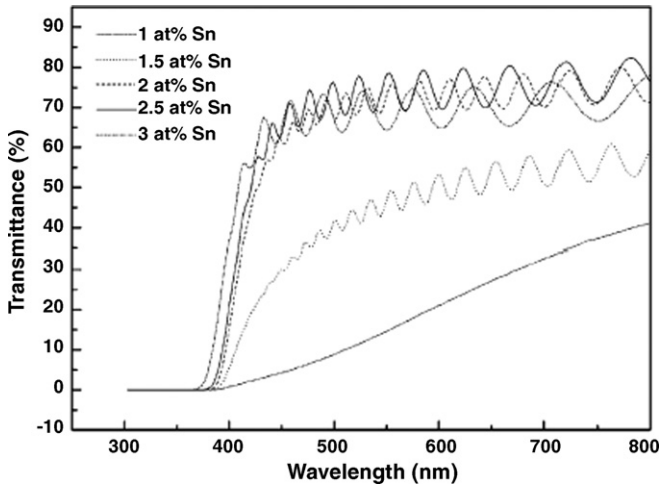

Fig. 6. Transmittance spectra as a function of wavelength in the range 300–800 nm for 1, 1.5, 2, 2.5 and 3 at.% of Sn-doped ZnO thin films.

The transmittance spectra, as a function of wavelength in the range of 300–800 nm for the five samples, are shown in Fig. 6. The average transmittance in the visible region is more than 80% while the concentration of Sn dopant is 2.5 at.% or less. Beyond the value, the transmittance decreases remarkably. The undulating shape of the transmission curves is caused by interference of the light in the film itself.

The optical energy gap (E_g) of the films was estimated from the optical measurements. The absorption coefficient (α) was calculated from the transmittance T and reflectance R with the relation [30]:

$$T = (1 - R^2)\,\exp(-\alpha d)$$

where R is the reflectance and d is the thickness of film. The optical energy gap of the films can be determined from the absorption coefficient of the films using the relation for parabolic bands [31]:

$$\alpha = A(h\nu - E_g)^{1/2}$$

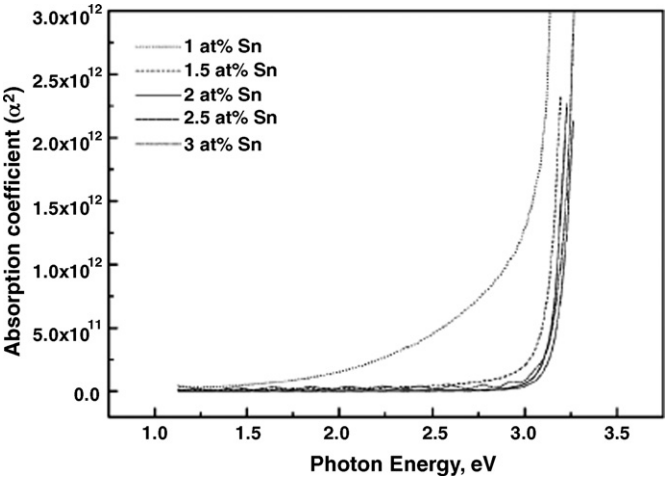

Fig. 7. Plot of $(\alpha)^2$ vs. the photon energy in the absorption region.

where A is the constant depending on the semiconductor material but not photon energy, and $h\nu$ is the incident photon energy. The plot of $(\alpha)^2$ versus the photon energy in the absorption region is shown in Fig. 7. According to the equation, the plot of $(\alpha)^2$ as a function of $h\nu$ results in a straight line whose intercept on the energy axis gives the value of E_g. It is noticed that E_g value at 2% of Sn dopant is approximately 3.18 eV, which was the maximum value obtained in this research.

4. Conclusion

The ZnO thin film can be easily deposited by successive immersions of the Pyrex glass substrate into a cold complex solution and then in hot water. The thickness of the film can be controlled by varying the number of successive immersions. Addition of more than 1.5% Sn as a dopant induces poisoning of the nucleation stage and hinders the formation of fine ZnO grains. With a nodular-shape dense appearance, the film produced from zinc containing complex having 1.5% Sn as precursor, is composed of even sized ZnO particles of 110–190 nm. The resistivity decreases with the increasing of the doping amount of tin. It can be concluded that the optimum concentration of Sn dopant in producing thin films containing fine grains with little resistivity is about 1.5%. The optical energy gap (E_g) increases with the increasing of the doping amount of Sn in zinc oxide films. The value of E_g ranges from 3.05 to 3.18 eV depending on the amount of Sn incorporated.

References

[1] H.L. Hartnagel, A.K. Jain, C. Jagadish, Semiconducting Transparent Thin Films, Paston Press, UK, 1995.
[2] K. Ellmer, K. Diesner, R. Wendt, S. Fiechter, Solid State Phenom. (1996) 51–52.
[3] S. Brehme, F. Fenske, W. Fuhs, E. Nebauer, M. Poschenrieder, B. Sells, I. Sieber, Thin Solid Films 342 (1996) 666–671.
[4] H. Sato, T. Minami, S. Takata, Thin Solid Films 220 (1992) 327–331.
[5] H.H. Woodbury, D.G. Thomas (Eds.), II–VI Semiconductor Compounds, Benjamin, New York, 1967, p. 244.
[6] D.G. Thomas, R. Dingle, J.D. Cuthbert, D.G. Thomas (Eds.), II–VI Semiconductor Compounds, Benjamin, New York, 1967, p. 863.
[7] B. Tell, J. Appl. Phys. 42 (1971) 2919–2923.
[8] D.B. Eason, G. Gantwell, Compd. Semicond. 8 (2002) 15–22.
[9] T. Minami, H. Nanto, S. Takata, Jpn. J. Appl. Phys. 23 (1984) L280.
[10] J. Hu, R.G. Gordon, Sol. Cells 30 (1991) 437–441.
[11] M. Joseph, H. Tabata, T. Kawai, Appl. Phys. Lett. 74 (1999) 2534–2539.
[12] A. Kuroyanagi, Jpn. J. Appl. Phys. 28 (1989) 219–225.
[13] J.R. LaGraff, G.Z. Pan, K.N. Tu, Physica C 338 (2000) 269–283.
[14] H. Gopalaswamy, P.J. Reddy, Semicond. Sci. Technol. 5 (1990) 980–986.
[15] J. Aranovich, A. Ortiz, R.H. Bube, J. Vac. Sci. Technol. 16 (1979) 994–1003.
[16] J.S. Kim, H.J. Marzouk, P.J. Reocroft Jr., C.E. Hamrin, Thin Solid Films 217 (1992) 133–138.
[17] M. Ristov, G.J. Grozdanov, M. Mitreski, Thin Solid Films 149 (1987) 65–70.
[18] K. Ramamoorthy, C. Sanjeeviraja, M. Jayachadran, K. Sankaranarayanan, D. Bhattacharaya, L.M. Kukreja, J. Cryst. Growth 226 (2001) 281–287.
[19] P. Mitra, A.P. Chatterjee, H. Maiti, J. Mater. Sci. 9 (1998) 441–446.
[20] K. Ramamoorthy, M. Arivanandhan, K. Sankaranarayanan, C. Sanjeeviraja, Mater. Chem. Phys. 85 (2004) 257–262.
[21] M.R. Vaezi, S.K. Sadrnezhaad, Mater. Sci. Technol. 22 (2006) 308–314.
[22] M.R. Vaezi, S.K. Sadrnezhaad, Mater. Des. 28 (2007) 1065–1070.
[23] S.K. Sadrnezhaad, M.R. Vaezi, Mater. Sci. Eng. B 128 (2006) 53–57.
[24] E.J. Luna- Arredondo, A. Maldonado, R. Asomoza, D.R. Acosta, M.A. Melendez- Lira, M. de la L. Olvera, Thin Solid Films 490 (2005) 132–136.
[25] Handbook of Nanophase and Nanostructured Materials, vol. I.
[26] A. Urbieta, P. Fernandez, J. Piqueras, E. Vasco, C. Zaldo, J. Optoelectron. Adv. Mater. 6 (1) (2004) 183–188.
[27] T. Nutz, U. Zum Felda, M. Haase, J. Chem. Phys. 110 (1999) 12142.
[28] Y.S. Chang, J.M. Ting, Thin Solid Films 398–399 (2001) 29–34.
[29] O. Hamad, G. Braunstein, H. Patil, N. Dhere, Thin Solid Films 489 (2005) 303–309.
[30] M. Digiulto, G. Micocei, R. Rella, P. Siciliano, A. Lepore, Thin Solid Films 148 (1987) 237–243.
[31] D. Jiles, Introduction to the Electronic Properties of Materials, Chapman and Hall, 1994, p. 1 (Chapter 9).